Stochastic Coherent Adaptive Large-Eddy Simulation with explicit filtering

Giuliano De Stefano[1] and Oleg V. Vasilyev[2]

[1] Dipartimento di Ingegneria Aerospaziale e Meccanica, Seconda Università di Napoli, via Roma 29, I 81031 Aversa, Italy giuliano.destefano@unina2.it

[2] Department of Mechanical Engineering, University of Colorado, Engineering Center, ECME 126, CO 80309 Boulder, USA oleg.vasilyev@colorado.edu

Summary. Stochastic Coherent Adaptive Large-Eddy Simulation is a novel approach to the numerical simulation of turbulence, based upon the wavelet thresholding filter, where the coherent energetic eddies are solved while modelling the influence of the less energetic background flow. In this study, in order to examine the quality and reliability of the method, additional explicit wavelet filtering is introduced by considering two different filtering levels: the physical level, which controls the turbulence model, and the numerical level that is responsible for the accuracy of the numerical simulations. The theoretical basis for explicit filtering and consistent dynamic modelling is given, and some preliminary numerical experiments are presented.

Key words: Adaptive Large-Eddy Simulation, Explicit/Implicit Wavelet Filtering, Dynamic modelling

1 Introduction

The stochastic coherent adaptive large-eddy simulation (SCALES) method is a novel approach to the numerical simulation of turbulence, where the more energetic coherent eddies are solved, while modelling the effect of the less energetic background flow [1]. The formal decomposition between resolved coherent and residual coherent/incoherent motions is obtained through the application of wavelet-based filtering. The space-time evolution of the resolved coherent velocity field is governed by the wavelet-filtered Navier-Stokes equations, where – similarly to any other LES approach – the effect of the unknown residual stresses is modelled.

In order to solve the SCALES governing equations in a computationally efficient manner, the dynamically adaptive wavelet collocation method (AWCM) is used, e.g. [2]. The AWCM procedure is a variable high-order finite-difference method that exploits the same wavelet-based filter to automatically adapt the computational grid to the numerical solution, in both location and scale.

To date, the filtering effect induced by the use of the AWCM has been exploited to implicitly define the filtered-velocity in the SCALES approach, without performing any additional explicit filtering operation. Along this line, the residual stresses have been referred to and treated as subgrid-scale (SGS) stresses, e.g. [3]. It is worth noting that the fundamental issue regarding the interaction between LES filtering, SGS modelling, and numerical errors becomes even more important in the SCALES approach, where the numerical solver allows for the automatic mesh refinement in flow regions with inadequate SGS dissipation.

In this study, in order to examine the quality and reliability of the SCALES methodology, the additional explicit wavelet-filtering procedure is introduced. That is, two different thresholding levels are clearly considered: the physical level, which controls the turbulence model, and the numerical level that is solely responsible for the accuracy of the numerical method. The theoretical basis for SCALES with explicit filtering is given and some preliminary numerical experiments are carried out for decaying homogeneous turbulence at moderate Reynolds-number.

2 Explicit wavelet-filtering approach

2.1 Wavelet-filtered velocity

The formal separation between resolved and unresolved flow structures is obtained through wavelet threshold filtering (WTF), which is performed by applying the wavelet-transform to the unfiltered velocity field, zeroing the wavelet coefficients below a given threshold, and transforming back to the physical space, e.g. [1, 4]. This way, the turbulent velocity field is decomposed into two different parts: a coherent more energetic velocity field and a residual less energetic coherent/incoherent one, i.e., $u_i = \overline{u_i}^{>\epsilon} + u'_i$, where $\overline{u_i}^{>\epsilon}$ stands for the wavelet-filtered velocity. Depending on the choice of the WTF level ϵ that is dictated by the desired turbulence resolution, a relatively small number of wavelets are retained in representing the filtered field $\overline{u_i}^{>\epsilon}$.

Table 1. Percentage of active wavelets and retained energy/enstrophy for different WTF levels

level ϵ	wavelets	energy	enstrophy
0.45	0.11%	97.8%	66.0%
0.35	0.26%	99.0%	78.4%
0.25	0.61%	99.5%	87.0%
0.15	1.86%	99.9%	95.1%

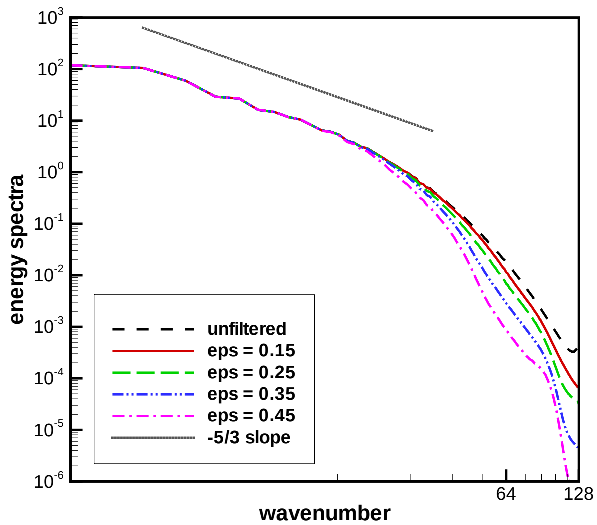

Fig. 1. Energy spectra for wavelet-filtered velocity fields at different levels of resolution (WTF level $\epsilon = 0.15$, 0.25, 0.35, and 0.45)

The high compression property of the wavelet-based decomposition is illustrated in Table 1, where the percentage of active wavelets and retained energy/enstrophy are reported as a function of the WTF level for a given turbulent velocity field. The field considered is a realization of a statistically stationary turbulent flow at $Re_\lambda = 126$ (λ being the Taylor microscale) provided by a pseudo-spectral DNS [5]. For instance, by retaining less than 1% of the 512^3 available wavelets, one is able to capture more than 99% of the energy and almost 90% of the DNS enstrophy.

Furthermore, one of the distinctive features of WTF stands in the ability to capture coherent energetic eddies of any size. For this reason, the small scale turbulence can be represented – at least partially – by the wavelet-filtered field. This is illustrated in Figure 1, where the energy spectra corresponding to different filtering levels are reported for the above mentioned DNS field.

2.2 Wavelet-filtered equations

The governing equations for SCALES of incompressible turbulent flows are represented by the following wavelet-filtered continuity and Navier-Stokes equations:

$$\frac{\partial \overline{u_i}^{>\epsilon}}{\partial x_i} = 0, \tag{1}$$

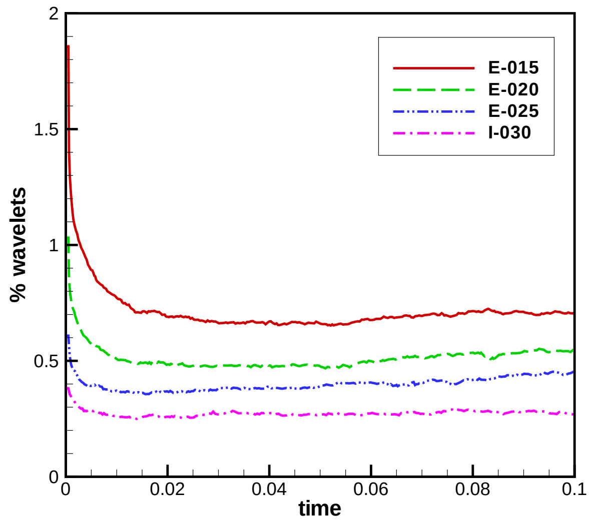

Fig. 2. Percent of retained wavelets for different numerical thresholds (labels as in Table 2)

$$\frac{\partial \overline{u_i}^{>\epsilon}}{\partial t} + \frac{\partial \overline{u_i}^{>\epsilon}\,\overline{u_j}^{>\epsilon}}{\partial x_j} = -\frac{1}{\rho}\frac{\partial \overline{p}^{>\epsilon}}{\partial x_i} + \nu \frac{\partial^2 \overline{u_i}^{>\epsilon}}{\partial x_j \partial x_j} - \frac{\partial \tau_{ij}}{\partial x_j}, \tag{2}$$

where the unknown subgrid-scale (SGS) stresses

$$\tau_{ij} = \overline{u_i u_j}^{>\epsilon} - \overline{u}_i^{>\epsilon}\,\overline{u}_j^{>\epsilon} \tag{3}$$

need modelling.

From the mathematical point of view, once the SGS stress tensor is given as a function of the resolved velocity $\overline{u_i}^{>\epsilon}$ and suitable initial conditions are provided, the SCALES governing equations can be solved using any numerical method. In practice, equation (2) is solved using the dynamically adaptive wavelet collocation method, where the WTF procedure is exploited to automatically adapt the computational grid to the numerical solution, in both location and scale, e.g. [2]. The use of the AWCM procedure involves an unavoidable built-in filtering effect associated to the wavelet numerical threshold ϵ_{g} that is used to control the numerical errors. When this induced filtering operation is exploited to unambiguously define the wavelet-filtered velocity assuming $\epsilon = \epsilon_{\mathrm{g}}$, there is no reason to discern between explicit and implicit wavelet-filtering, e.g. [3]. However, since the choice of a relatively high threshold level ϵ_{g} could affect the accuracy of the numerical simulations, alternatively, one can consider two different superimposed levels of filtering: explicit-filtering at ϵ and implicit-filtering at $\epsilon_{\mathrm{g}} < \epsilon$. The use of such an approach results in adding extra computational modes beyond the modes that are strictly

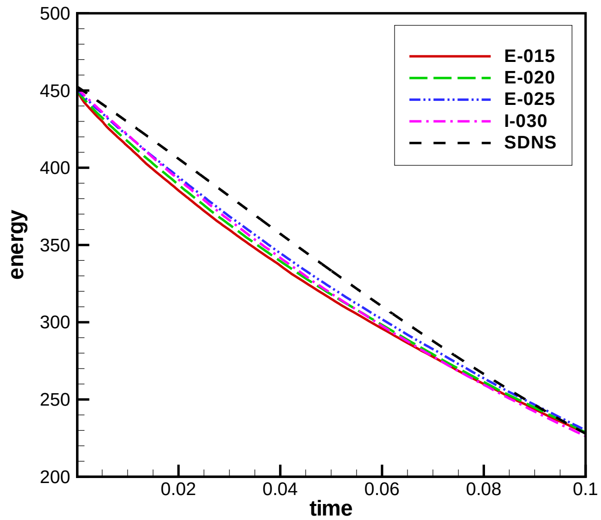

Fig. 3. Resolved kinetic energy for different numerical thresholds (labels as in Table 2)

necessary for the desired SCALES solution, but less than in simulations with smaller ϵ, since the energy cascade is broken by the model.

Considering SCALES with explicit filtering, the momentum equation can be written in the following explicit-filtered form

$$\frac{\partial \overline{u_i}^{>\epsilon}}{\partial t} + \frac{\partial \overline{\overline{u_i}^{>\epsilon}\,\overline{u_j}^{>\epsilon}}^{>\epsilon}}{\partial x_j} = -\frac{1}{\rho}\frac{\partial \overline{p}^{>\epsilon}}{\partial x_i} + \nu \frac{\partial^2 \overline{u_i}^{>\epsilon}}{\partial x_j \partial x_j} - \frac{\partial \overline{\tau}_{ij}^{>\epsilon}}{\partial x_j}, \qquad (4)$$

where

$$\overline{\tau}_{ij}^{>\epsilon} = \overline{u_i u_j}^{>\epsilon} - \overline{\overline{u}_i^{>\epsilon}\,\overline{u}_j^{>\epsilon}}^{>\epsilon} \qquad (5)$$

can be referred to as subfilter-scale (SFS) stresses.

2.3 Subfilter-scale model

The closure models used in the past for SCALES of turbulent flows should be consistently revised in order to be applied in conjunction with explicit-filtering. For instance, following the eddy-viscosity dynamic Smagorinsky modelling approach proposed in [6], the deviatoric part of the SFS turbulent stress tensor is approximated as

$$\overline{\tau}_{ij}^{>\epsilon *} \cong -2\overline{C_S \Delta^2 \epsilon^2 \left|\overline{S}^{>\epsilon}\right| \overline{S}_{ij}^{>\epsilon}}^{>\epsilon}, \qquad (6)$$

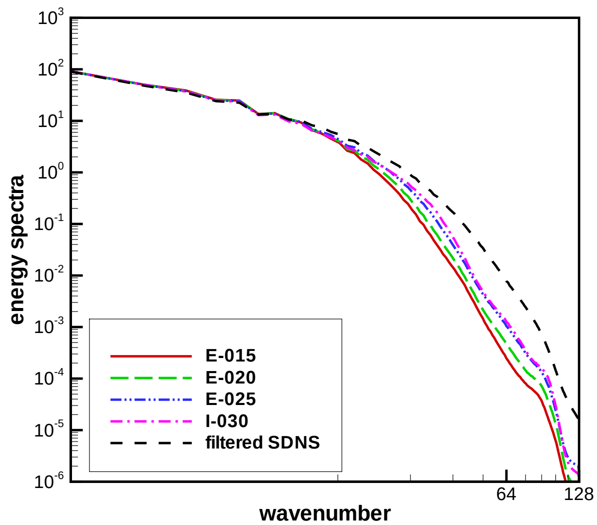

Fig. 4. Energy spectra at $t = 0.05$ for different numerical thresholds (labels as in Table 2)

where $\overline{S_{ij}}^{>\epsilon} = 1/2\left(\partial\overline{u_i}^{>\epsilon}/\partial x_j + \partial\overline{u_j}^{>\epsilon}/\partial x_i\right)$ is the filtered rate-of-strain tensor, $\left|\overline{S}^{>\epsilon}\right| = \left(2\overline{S_{ij}}^{>\epsilon}\overline{S_{ij}}^{>\epsilon}\right)^{1/2}$, and Δ is the characteristic explicit-filter length-scale. The residual stress tensor at the test-filter level is defined as the following analog of (5)

$$\overline{T}_{ij}^{>2\epsilon} = \overline{u_i u_j}^{>2\epsilon} - \overline{\overline{u}_i^{>2\epsilon}\,\overline{u}_j^{>2\epsilon}}^{>2\epsilon}, \tag{7}$$

where $\overline{(\cdot)}^{>2\epsilon}$ corresponds to the wavelet test filter at twice the threshold. Since the wavelet filter is a projection operator it satisfies $\overline{\overline{(\cdot)}^{>\epsilon}}^{>2\epsilon} \equiv \overline{(\cdot)}^{>2\epsilon}$. Therefore, by filtering (5) at the test filter level and combining it with (7), the following modified Germano identity for the known Leonard stresses is obtained:

$$\overline{L}_{ij}^{>2\epsilon} \equiv \overline{T}_{ij}^{>2\epsilon} - \overline{\tau_{ij}}^{>2\epsilon} = \overline{\overline{u_i}^{>\epsilon}\overline{u_j}^{>\epsilon}}^{>2\epsilon} - \overline{\overline{u_i}^{>2\epsilon}\,\overline{u_j}^{>2\epsilon}}^{>2\epsilon}. \tag{8}$$

Exploiting the model (6) and the analogous relation for the test filtered SFS stresses that is

$$\overline{T}_{ij}^{>2\epsilon *} \cong -\overline{2C_S\Delta^2\left(2\epsilon\right)^2\left|\overline{S}^{>2\epsilon}\right|\overline{S}_{ij}^{>2\epsilon}}^{>2\epsilon}, \tag{9}$$

one obtains

$$\overline{2C_S\Delta^2\epsilon^2\left|\overline{S}^{>\epsilon}\right|\overline{S}_{ij}^{>\epsilon}}^{>2\epsilon} - \overline{2C_S\Delta^2\left(2\epsilon\right)^2\left|\overline{S}^{>2\epsilon}\right|\overline{S}_{ij}^{>2\epsilon}}^{>2\epsilon} = \overline{L}_{ij}^{>2\epsilon *}. \tag{10}$$

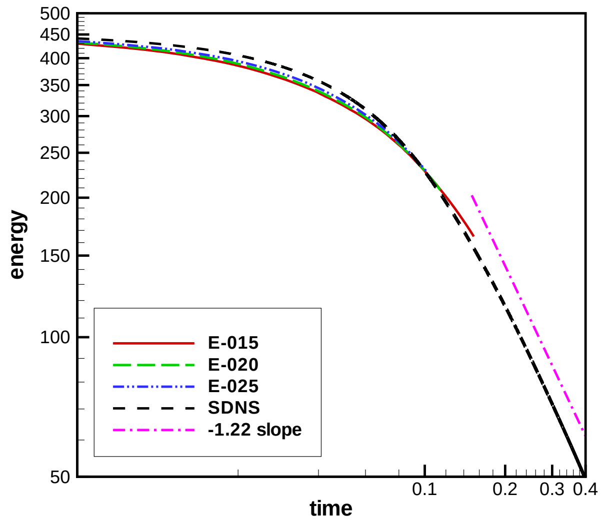

Fig. 5. Total dissipation for different numerical thresholds (labels as in Table 2)

Finally, a least square solution to (10) leads to the following equation for determining the Smagorinsky model coefficient:

$$2\epsilon^2 \Delta^2 C_S = \frac{\langle \overline{L}_{ij}^{>2\epsilon *} \overline{M}_{ij}^{>2\epsilon} \rangle}{\langle \overline{M}_{hk}^{>2\epsilon} \overline{M}_{hk}^{>2\epsilon} \rangle}, \tag{11}$$

where

$$\overline{M}_{ij}^{>2\epsilon} \equiv \overline{\left|\overline{S}^{>\epsilon}\right| \overline{S}_{ij}^{>\epsilon}}^{>2\epsilon} - 4\left|\overline{S}^{>2\epsilon}\right| \overline{S_{ij}}^{>2\epsilon}, \tag{12}$$

and $\langle \cdot \rangle$ denotes volume averaging that is performed to make the numerical solution stable.

3 Numerical experiments

In order to make some experiments for SCALES with explicit-filtering, the numerical simulation of incompressible homogeneous decaying turbulence is considered. The initial velocity field is provided by the above-mentioned statistically steady pseudo-spectral DNS solution at $Re_\lambda = 126$ that is obtained by solving the unfiltered Navier-Stokes equations, supplied with the random forcing scheme of Eswaran & Pope [8], with 256^3 Fourier modes. It is worth noting that the initial Reynolds-number is moderately high to allow a clear inertial scaling in the energy spectrum, as illustrated in Figure 1. The same pseudo-spectral code with the same resolution is used to produce a reference DNS solution for the decaying case (for discussion SDNS) as in [5].

Due to the finite difference nature of the wavelet-based solver, the initial SCALES resolution is doubled in each direction with respect to SDNS, in order to retain approximately the same initial energy content. For this reason, SCALES is run using a maximum resolution corresponding to 512^3 grid points (or, equivalently, wavelets). However, the actual number of wavelets used in the simulation is very low with respect to the above maximum value, owing to the high compression property of the wavelet-transform-based method discussed in Section 2.1. In addition, due to the decaying nature of the turbulent flow considered, a great number of wavelets is only required during the initial period, with a gradual decrease of the necessary level of numerical resolution as turbulence decays.

In this preliminary study, a number of calculations are performed for a given explicit WTF level, which is $\epsilon = 0.30$, and different numerical thresholds, ranging from $\epsilon_{\mathrm{g}} = 0.25$ down to $\epsilon_{\mathrm{g}} = 0.15$. The wavelet-filter at threshold ϵ is explicitly applied upon the resolved velocity field step-by-step during the simulation, which is practically equivalent to solving (4). Given ϵ, with the progressive improvement of the numerical accuracy, a grid-independent SCALES solution is approached for decreasing ϵ_{g}. This way, one can examine the pure combined effect of "physical" filtering and SGS modelling.

Some interesting results are illustrated for a time interval corresponding to approximately one SDNS initial eddy-turnover time. This short time is however sufficient to have a significant decay in the Reynolds-number that becomes $Re_\lambda \cong 72$. As further reference, the SCALES solution corresponding to $\epsilon_{\mathrm{g}} = 0.30$ without any explicit filtering is considered in the following (for discussion I-030). All the solutions presented are summarized in Table 2.

As expected, the number of wavelets retained in the calculation increases with the decrease of ϵ_{g}. However, even for the smallest value of ϵ_{g}, the percent of active wavelets is less than 1% of the total number of available wavelets, as illustrated in Figure 2. The energy decay for the different solutions is reported in Figure 3, while the energy spectra at a given time instant ($t = 0.05$) are illustrated in Figure 4. The time histories of total dissipation (resolved plus modelled) and modelled dissipation alone are depicted in Figures 5 and 6, respectively. Finally, in Figure 7 the evolution of the Reynolds-number is reported.

Table 2. SCALES calculations performed

label	ϵ_{g}	ϵ	explicit
E-015	0.15	0.30	yes
E-020	0.20	0.30	yes
E-025	0.25	0.30	yes
I-030	0.30	0.30	no

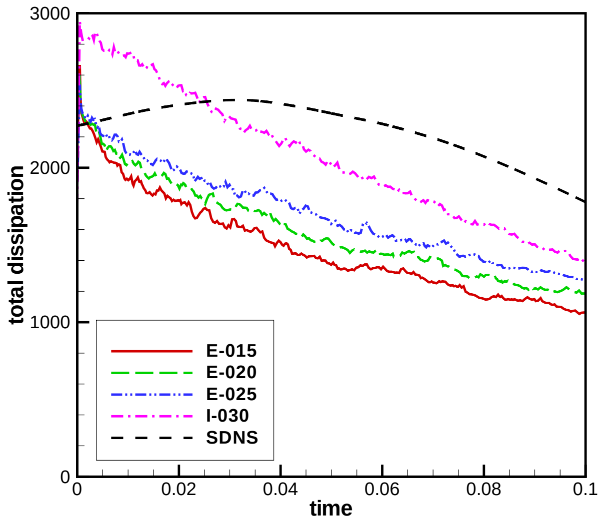

Fig. 6. Modelled dissipation for different numerical thresholds (labels as in Table 2)

For decreasing ϵ_{g}, the SCALES solution appears to depart from SDNS, approaching a grid-independent solution that represents the ideal evolution of the wavelet-filtered velocity field corresponding to the most energetic coherent eddies (as defined by the prescribed WTF level). An even lower numerical threshold should be considered to make this behavior more evident. Given ϵ, the SFS dissipation provided by the modelling procedure does not depend upon the grid resolution determined by the choice of ϵ_{g}, while the resolved dissipation tends to be lower, corresponding to the reduced enstrophy contained in the explicitly-filtered field. In the coarse-grid case (I-030), in absence of explicit-filtering ($\epsilon = \epsilon_{\mathrm{g}}$), the model automatically compensates for the lack of dissipation owing to the adaptive nature of the SCALES approach. However, in this case the picture becomes very complex and, in order to make it possible to better discern between the filtering and the numerical issues, the explicit-filtering procedure seems preferable.

4 Concluding remarks

In this work, the SCALES method is applied with superimposed explicit filtering. The study of the effect of numerical thresholding level on the accuracy and computational efficiency of SCALES is carried out. The explicit filtering allows the analysis of the quality and reliability of SCALES solutions with

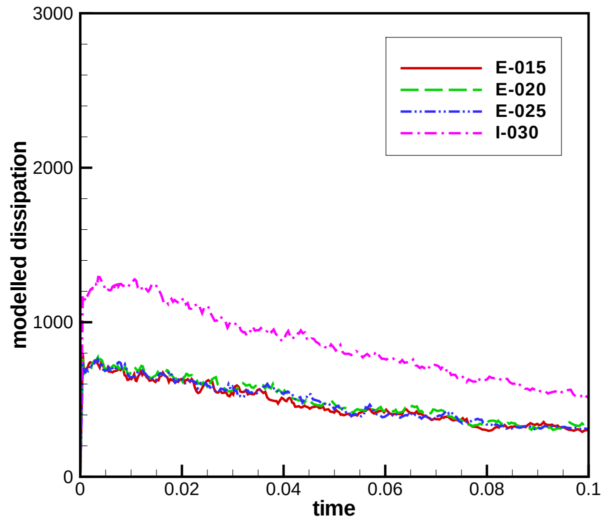

Fig. 7. Taylor Reynolds-number for different numerical thresholds (labels as in Table 2)

respect to ideal grid-independent calculations, thus enhancing our knowledge about the strong interactions between wavelet-compression and modelled turbulent dissipation in the wavelet-based numerical simulations of turbulence. Another possibility that will be examined in the future consists in varying the SFS threshold ϵ for a given very small value of ϵ_g. The use of a smaller SFS thresholding level would increase the number of resolved coherent structures, and the influence of the model would become less important, since the coherent eddies dynamics would be captured by the resolved modes.

References

1. Goldstein D E, Vasilyev O V (2004) Phys Fluids 16:2497–2513
2. Vasilyev O V, Kevlahan N K-R (2005) J Comp Phys 206:412–431
3. De Stefano G, Vasilyev O V, Goldstein D E (2008) Phys Fluids 20:045102.1–14
4. Farge M, Schneider K, Kevlahan N K-R (1999) Phys Fluids 11:2187–2201
5. De Stefano G, Goldstein D E, Vasilyev O V (2005) J Fluid Mech 525:263–274
6. Goldstein D E, Vasilyev O V, Kevlahan N K-R (2005) J Turbul 6:1–20
7. De Stefano G, Vasilyev O V (2004) Theoret Comput Fluid Dynamics 18:27–41
8. Eswaran V, Pope S B (1988) Comput Fluids 16:257–278